Neurobiology of Aging 84 (2019) 158–165

Contents lists available at ScienceDirect

Neurobiology of Aging

journal homepage: www.elsevier.com/locate/neuaging

High dilated perivascular space burden: a new MRI marker for risk of intracerebral hemorrhage

Marie-Gabrielle Duperron [a], Christophe Tzourio [a,b], Sabrina Schilling [a], Yi-Cheng Zhu [c], Aïcha Soumaré [a], Bernard Mazoyer [d], Stéphanie Debette [a,e,*]

[a] Univ. Bordeaux, Inserm U1219, Bordeaux Population Health Research Center, Bordeaux, France
[b] CHU de Bordeaux, Pole de santé publique, Service d'information médicale, Bordeaux, France
[c] Department of Neurology, Pekin Union Medical College Hospital, Beijing, China
[d] Univ. Bordeaux, Institut des Maladies Neurodégénératives, Bordeaux, France
[e] CHU de Bordeaux, Department of Neurology, Bordeaux, France

ARTICLE INFO

Article history:
Received 31 January 2019
Received in revised form 24 July 2019
Accepted 31 August 2019
Available online 10 September 2019

Keywords:
Cerebrovascular disease
Stroke
Ischemic stroke
Intracranial hemorrhage
Magnetic resonance imaging
Epidemiology

ABSTRACT

Commonly observed in older community persons, dilated perivascular spaces (dPVSs) are thought to represent an emerging MRI marker of cerebral small vessel disease, but their clinical significance is uncertain. We examined the longitudinal relationship of dPVS burden with risk of incident stroke, ischemic stroke, and intracerebral hemorrhage (ICH) in the 3C-Dijon population-based study (N = 1678 participants, mean age 72.7 ± 4.1 years) using Cox regression. dPVS burden was studied as a global score and according to dPVS location (basal ganglia, white matter, hippocampus, brainstem) at the baseline. During a mean follow-up of 9.1 ± 2.6 years, 66 participants suffered an incident stroke. Increasing global dPVS burden was associated with a higher risk of any incident stroke (hazard ratio [HR], 1.24; 95% CI, [1.06–1.45]) and of incident ICH (HR, 3.12 [1.78–5.47]), adjusting for sex and intracranial volume. Association with ICH remained significant after additionally adjusting for vascular risk factors and for other cerebral small vessel disease MRI markers. High dPVS burden in basal ganglia and hippocampus, but not in white matter or brainstem, were associated with higher risk of any stroke and ICH.

1. Introduction

Perivascular spaces are physiological fluid-filled structures surrounding vessel walls, as they run from the subarachnoid space through the brain parenchyma, with an MRI signal identical to cerebrospinal fluid (CSF) (Kwee and Kwee, 2007). Quantifiable on brain MRI, dilated perivascular spaces (dPVSs), or Virchow-Robin spaces, are an emerging MRI marker of cerebral small vessel disease (cSVD) (Mestre et al., 2017; Potter et al., 2015; Wardlaw et al. 2013b).

dPVSs are considered one of the earliest neuroimaging findings in cSVD. Although this is partly debated (Bacyinski et al., 2017), dPVSs may be part of the "glymphatic" system, involved in waste clearance (e.g., of beta amyloid peptide) and blood flow regulation (Jessen et al., 2015; Mestre et al., 2017). dPVS burden is associated with advancing age, hypertension (Yao et al., 2014; Zhu et al., 2010a), and other MRI markers of cSVD, including white matter hyperintensities of presumed vascular origin (WMH) and covert MRI-defined lacunes (Potter et al., 2015; Yakushiji et al., 2014; Zhu et al., 2010a).

The clinical significance and pathophysiology of dPVSs remain unclear. Although some studies have suggested an association of high dPVS burden with increased risk of dementia and cognitive decline (Francis et al., 2019; MacLullich et al., 2004; Passiak et al., 2019; Zhu et al., 2010b), results need to be confirmed in larger samples. To our knowledge, only one study in the general population examined the association of dPVS burden with incident stroke risk. The authors found an association of dPVS burden with an increased risk of any stroke, only for participants in the highest tertile of blood pressure, after adjusting for vascular risk factors (Gutierrez et al., 2017). The association of dPVS burden with stroke subtypes has not been explored in the general population.

We examined whether high dPVS burden is associated with increased risk of incident stroke, ischemic stroke, and intracerebral hemorrhage (ICH) in the population-based 3C-Dijon study.

2. Methods

The data that support the findings of this study are available from the corresponding author on reasonable request.

* Corresponding author at: Bordeaux University, 146 rue Léo-Saignat, 33076 Bordeaux, France. Tel.: +33557571659; fax: +33547304209.
E-mail address: stephanie.debette@u-bordeaux.fr (S. Debette).

0197-4580/$ – see front matter
https://doi.org/10.1016/j.neurobiolaging.2019.08.031

2.1. Study population

The 3C-Dijon study is a longitudinal population-based cohort study (The 3C-Study Group, 2003). Briefly, 4931 noninstitutionalized persons aged 65 years or older were recruited from the electoral rolls of Dijon, France, between March 1999 and March 2001. Participants are virtually all of European ancestry. Participants enrolled between June 1999 and September 2000 who were younger than 80 years (N = 2763) were proposed to undergo a brain MRI at the baseline. Participation rate was high (82.7%), but only 1924 MRI examinations were performed because of financial limitations. After exclusion of participants with brain tumor (N = 8), stroke (N = 83), or dementia (N = 8) at the time of MRI, participants with technical limitations preventing reliable assessment of dPVS burden (N = 45) or intracranial volume (ICV) (N = 75), and participants with no follow-up for stroke (N = 27), the baseline sample comprised 1678 participants. The study protocol was approved by the Ethical Committee of the University Hospital of Kremlin-Bicêtre. All participants provided written informed consent.

2.2. Brain MRI acquisition

MRI acquisition was performed on a 1.5-Tesla Magnetom scanner (Siemens); a 3-dimensional (3D) high-resolution T1-weighted, as well as T2- and PD- (proton density) weighted brain imaging were acquired (Supplementary Methods).

2.3. Rating of dPVSs

dPVSs were rated in 4 main locations (basal ganglia [BG], white matter [WM], hippocampus, and brainstem) by an experienced reader (Y-C.Z). Intrarater agreement (N = 100 MRI) was high (k = 0.77 for basal ganglia, and k = 0.75 for white matter) (Zhu et al., 2010a). dPVSs were defined as lesions with a CSF-like signal (hypointense on T1 and hyperintense on T2) of round, ovoid, or linear shape with a maximum diameter <3 mm, having smooth delineated contours, and located in areas supplied by perforating arteries. Lesions fulfilling the same criteria except for a diameter ≥3 mm were carefully examined in the 3 planes (shape, signal intensity) to differentiate them from covert MRI-defined lacunes and WMH. Only lesions with a typical vascular shape (including cystic lesions with an extension of vascular shape) and that followed the orientation of perforating vessels were considered as dPVSs (Zhu et al., 2010a).

In the BG, the slice containing the greatest number of dPVSs was used for the rating on a 4-grade score: grade 1 for <5 dPVSs; grade 2 for 5–10 dPVSs; grade 3 for >10 dPVSs but still numerable; grade 4 for innumerable dPVSs resulting in a cribriform change in the BG (Fig. 1). In the WM, dPVSs were also rated using a 4-grade score:

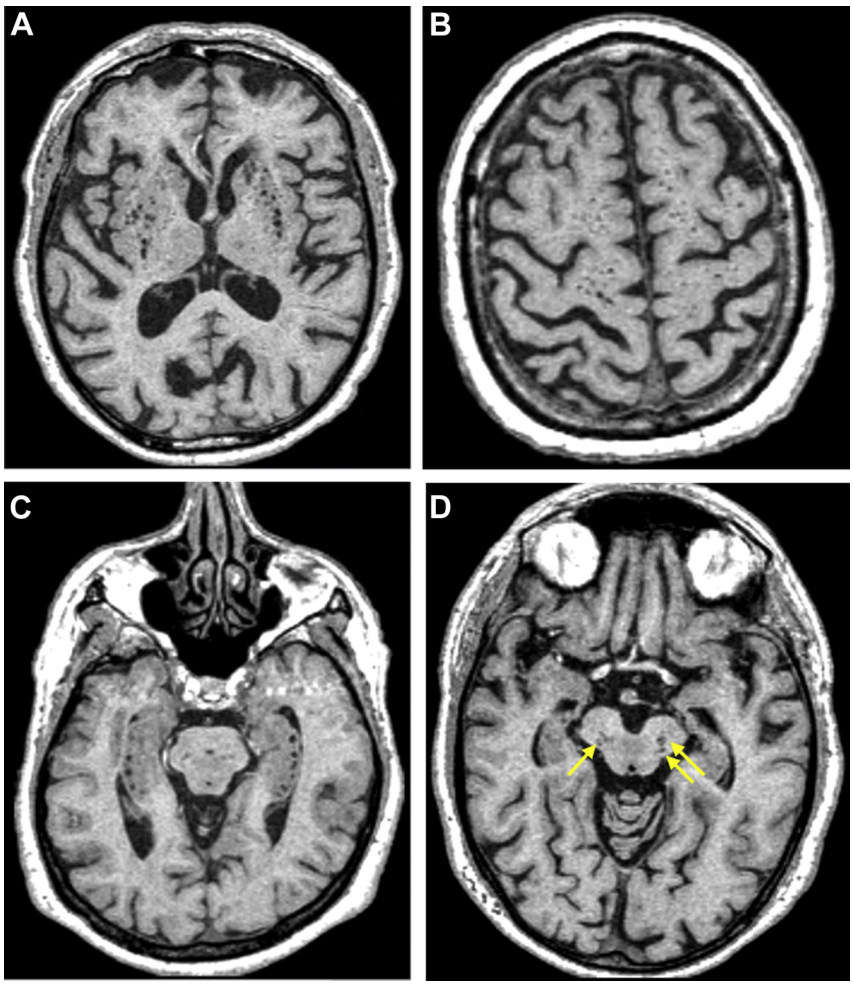

Fig. 1. Axial T1-weighted images of high dilated perivascular space burden. High dilated perivascular space burden in basal ganglia (A, grade 4) white matter (B, grade 4), hippocampus (C), and mesencephalon (D), 3C-Dijon study.

grade 1 for <10 dPVSs in the total WM; grade 2 for ≥10 dPVSs in the total WM and <10 in the slice containing the greatest number of dPVSs; grade 3 for 10–20 dPVSs in the slice containing the greatest number of dPVSs; grade 4 for >20 dPVSs in the slice containing the greatest number of dPVSs (Fig. 1) (Zhu et al., 2010a). In the hippocampus and brainstem, dPVS count was reported; participants with the largest number of dPVSs seen in <2% of the population were grouped with the previous category to better fit the statistical model, leading to a variable ranging between 0 and 5 in the hippocampus and between 0 and 6 in the brainstem.

A global dPVS burden variable was constructed by summing up dPVS grades in BG and WM, and adding 1 point for the presence of ≥1 dPVS in the hippocampus, and 1 point for the presence of ≥1 dPVS in the brainstem. Owing to the small number of participants in the highest categories, these were combined (global score ≥8), leading to a global dPVS score ranging from 2 to 8. The global variable was normally distributed on visual inspection (Supplementary Methods). Extensive global dPVS burden was defined by the cutoff closest to the top-quartile (score ≥7).

2.4. Other MRI measurements

WMH volume (WMHV) was measured using a fully automated and validated procedure (Maillard et al., 2008). Covert MRI-defined brain infarcts were defined as focal lesions ≥3 mm with the same signal characteristics as CSF on all sequences, not associated with any history of stroke (exclusion criterion). Covert MRI-defined lacunes were defined as covert MRI-defined brain infarcts with a diameter between 3 and 15 mm, located in the BG, brainstem, or WM (Zhu et al., 2010a). The ICV was estimated using voxel-based morphometry by summing up gray matter, WM, and CSF volumes (Lemaitre et al., 2005). The brain parenchymal fraction was estimated by summing up gray and white matter volume and dividing by the ICV.

2.5. Stroke assessment

Incident stroke was defined as a new focal neurological deficit of sudden onset, of presumed vascular origin, that persisted for >24 hours, or leading to death. Diagnosis of stroke, stroke classification (ischemic stroke, ICH, or unspecified), and ischemic stroke subtyping (cardioembolic, large-artery occlusion, or small-artery occlusion) was carried out by an expert panel according to the criteria of the World Health Organization (The World Health Organization MONICA Project, WHO Monica Project Principal Investigators, 1988). Of note, large-artery ischemic strokes were not studied separately in association with dPVS burden because there were too few events in this category. Strokes were defined as fatal if followed by death within 28 days. Incident stroke events were ascertained and classified blinded to the baseline dPVS rating.

2.6. Statistical analyses

Global burden of dPVSs and dPVS burden in hippocampus and brainstem were studied as continuous variables, and dPVS burden in BG and WM as a dichotomized variable (grade 3–4/1–2). Because WMHV had a skewed distribution, we used natural log-transformed values (natural log of [Ln (WMHV+1)] (Verhaaren et al., 2015). Covert MRI-defined lacunes were studied as dichotomous variables (at least one lacune vs. none).

To study the association between dPVS burden and incident stroke, we used a Cox regression model with age as a time scale. Follow-up started on the date of the baseline brain MRI and occurrence of a first stroke was used as an endpoint. Participants

Table 1
Baseline characteristics of the study population

Characteristics	Total population (N = 1678)	dPVS (global) ≥7 (N = 218)	dPVS (global) <7 (N = 1460)
Age at MRI, years, mean ± standard deviation	72.7 ± 4.1	74.1 ± 4.1[b]	72.5 ± 4.1[b]
Women, N (%)	1026 (61.1)	115 (52.8)[a]	911 (62.4)[a]
Educational level >baccalaureate[c]	613 (36.6)	90 (41.3)	523 (35.9)
Hypertension status[d]	1286 (76.7)	188 (86.2)[a]	1098 (75.2)[a]
Antihypertensive treatment intake	714 (42.6)	125 (57.3)[b]	589 (40.3)[b]
Systolic blood pressure, mm Hg	148.8 ± 22.6	153.7 ± 21.0[a]	148.0 ± 22.8[a]
Diastolic blood pressure, mm Hg	85.0 ± 11.5	87.2 ± 11.4[a]	84.6 ± 11.5[a]
Pulse pressure, mm Hg	63.8 ± 17.1	66.6 ± 16.6	63.4 ± 17.2
Antithrombotic drug intake	623 (37.1)	95 (43.6)	528 (36.2)
Body mass index, kg/m^2	25.4 ± 3.8	25.4 ± 3.6	25.4 ± 3.8
Current smoker	96 (5.7)	14 (6.4)	82 (5.6)
Diabetes mellitus[e]	136 (8.2)	19 (8.7)	117 (8.1)
Hypercholesterolemia[f]	945 (56.7)	119 (54.6)	826 (57.0)
Lipid lowering treatment intake	552 (32.9)	71 (32.6)	481 (33.0)
Total cholesterol, mmol/L	5.8 ± 0.9	5.7 ± 0.9	5.8 ± 0.9
Low-density lipoprotein, mmol/L	3.6 ± 0.8	3.5 ± 0.8	3.6 ± 0.8
Triglycerides, mmol/L	1.2 ± 0.5	1.2 ± 0.6	1.2 ± 0.5
HDL cholesterol, mmol/L	1.7 ± 0.4	1.6 ± 0.4	1.7 ± 0.4
History of cardiovascular disease[g]	67 (4.0)	11 (5.1)	56 (3.8)
Apolipoprotein E ε4 carrier status	366 (22.0)	43 (19.7)	323 (22.3)
Intracranial volume, cm^3	1363.7 ± 135.3	1388.0 ± 136.1	1360.1 ± 134.8
Covert MRI-defined lacunes	121 (7.3)	45 (21.3)[b]	76 (5.3)[b]
Covert MRI-defined brain infarct	146 (8.7)	52 (23.9)[b]	94 (6.4)[b]
White matter hyperintensity volume, cm^3	5.5 ± 5.0	7.8 ± 5.6[b]	5.2 ± 4.8[b]

Logistic regression between participants with a global dPVS burden score ≥7 versus <7 adjusted for age and sex.
Key: dPVS, dilated perivascular space.
[a] $p < 0.05$.
[b] $p < 0.0001$.
[c] Final high-school degree in France;
[d] Systolic blood pressure ≥140 mm Hg or diastolic blood pressure ≥90 mm Hg or antihypertensive drugs;
[e] Blood glucose ≥7 mmol/L ± antidiabetic drugs;
[f] Total cholesterol level ≥6.2 mmol/L;
[g] Including myocardial infarction, peripheral artery disease, cardiac and vascular surgery (participants with stroke excluded).

known to be stroke-free were right censored at the time of non-stroke death or at the time of their last follow-up. For analyses of association with incident stroke subtypes, participants with alternative subtypes were censored at the time of event.

Participants' demographic and cardiovascular risk factors were assessed at the baseline (Supplementary Methods). To adjust for potential confounding factors, we constructed 5 models: model 1 adjusted for sex and ICV, model 2 additionally adjusted for vascular risk factors (hypertension, diabetes, hypercholesterolemia, current smoking status, and body mass index), model 3 adjusted for the same variables as in model 1 and for APOEε4-carrier status, model 4 adjusted for the same variables as in model 1 and for covert MRI-defined lacunes and WMHV and model 5 adjusted for the same variables as in model 2 and for antithrombotic drug intake. Analyses were corrected for multiple testing, accounting for the 4 dPVS locations (significance threshold after correction for multiple testing: $p < 0.0125$). The trend in risk of incident stroke across dPVS grades in the BG assigned with ordered natural numbers (1, 2, 3, and 4) was tested using the Cox proportional hazards model. We searched for an effect modification by sex, hypertension, median age, and APOEε4-carrier status. We verified the linearity hypothesis with a restricted cubic spline model (Desquilbet and Mariotti, 2010) and the proportional hazard assumption using proportionality tests that assess the statistical significance of interaction terms between time and the variables in the model. We also performed cumulative incidence graphs adjusted for age, sex, and total intracranial volume and stratified on global extensive dPVS burden (top quartile vs. the rest). The Fine and Gray method has been used to model the cumulative incidence of intracerebral hemorrhage to take into account competitive risks with other stroke subtypes.

Analyses were performed using Statistical Analyses System software version 9.3 (SAS Institute, Inc, Cary, NC).

3. Results

For the 1678 participants, the average age at the baseline was 72.7 years (standard deviation 4.1) and 61.1% were women (Table 1). Over a mean follow-up period of 9.1 ± 2.6 years, 66 participants (3.9%) developed an incident stroke (52 ischemic strokes, 10 ICH, and 4 strokes of unspecified type). Of the 52 incident ischemic strokes, the subtype was cardioembolic (N = 14), small-artery occlusion (N = 11), large artery (N = 1), other etiologies (N = 2), and undetermined (N = 24). Among the 10 participants who developed an ICH, 4 participants were treated by antithrombotic drugs during the follow-up before the event; and the ICH localization was deep in 4 participants, lobar in 1 participant, and undetermined in 5 participants. Of the 66 strokes, 10 were fatal, of which 4 were ischemic strokes (8% fatality rate) and 4 were ICHs (40% fatality rate).

All participants had some dPVSs. Of these, 218 (13%) had an extensive global dPVS burden. The presence of an extensive global dPVS burden was significantly associated with older age, hypertension, systolic and diastolic blood pressure, and antihypertensive drug intake, but not other vascular risk factors. We also observed a significant association of extensive global dPVS burden with covert MRI-defined lacunes and WMHV (Table 1).

Table 2
Association between dilated perivascular spaces burden and incident stroke

dPVS location	All strokes			Ischemic stroke			Intracerebral hemorrhage		
	n/N	HR [95% CI]	*p*-Value	n/N	HR [95% CI]	*p*-Value	n/N	HR [95% CI]	*p*-Value
Model 1[a]									
dPVS (global)	66/1678	1.24 [1.06–1.45]	**0.006**	52/1678	1.05 [0.88–1.26]	0.577	10/1678	3.12 [1.78–5.47]	**6.91×10^{-5}**
dPVS (basal ganglia)		2.28 [1.28–4.04]	**0.005**		1.30 [0.61–2.80]	0.496		11.47 [3.15–41.70]	**0.0002**
dPVS (white matter)		1.21 [0.70–2.09]	0.484		0.77 [0.39–1.54]	0.463		3.13 [0.90–10.86]	0.072
dPVS (hippocampus)		1.23 [1.07–1.42]	**0.004**		1.04 [0.87–1.26]	0.651		2.55 [1.69–3.86]	**7.95×10^{-6}**
dPVS (brain stem)		1.06 [0.94–1.21]	0.332		1.09 [0.95–1.26]	0.209		1.14 [0.83–1.55]	0.417
Model 2[b]									
dPVS (global)	66/1659	1.23 [1.05–1.44]	**0.009**	52/1659	1.03 [0.86–1.24]	0.719	10/1659	3.63 [1.93–6.83]	**6.44×10^{-5}**
dPVS (basal ganglia)		2.23 [1.26–3.97]	**0.006**		1.25 [0.58–2.69]	0.564		11.98 [3.25–44.11]	**0.0002**
dPVS (white matter)		1.19 [0.69–2.05]	0.531		0.75 [0.37–1.49]	0.408		3.38 [0.96–11.88]	0.057
dPVS (hippocampus)		1.23 [1.07–1.42]	**0.005**		1.03 [0.86–1.24]	0.753		2.84 [1.82–4.45]	**4.84×10^{-6}**
dPVS (brain stem)		1.06 [0.94–1.20]	0.337		1.09 [0.95–1.25]	0.231		1.14 [0.84–1.56]	0.407
Model 3[c]									
dPVS (global)	66/1666	1.24 [1.06–1.45]	**0.008**	52/1666	1.04 [0.87–1.25]	0.655	10/1666	3.11 [1.77–5.46]	**7.30×10^{-5}**
dPVS (basal ganglia)		2.27 [1.28–4.02]	**0.005**		1.30 [0.60–2.78]	0.507		11.46 [3.16–41.64]	**0.0002**
dPVS (white matter)		1.20 [0.69–2.06]	0.516		0.76 [0.38–1.52]	0.437		3.10 [0.89–10.76]	0.074
dPVS (hippocampus)		1.23 [1.07–1.42]	**0.005**		1.04 [0.86–1.25]	0.684		2.56 [1.70–3.87]	**7.96×10^{-6}**
dPVS (brain stem)		1.06 [0.93–1.20]	0.378		1.09 [0.94–1.25]	0.249		1.14 [0.83–1.55]	0.422
Model 4[d]									
dPVS (global)	66/1649	1.13 [0.96–1.34]	0.134	52/1649	0.97 [0.81–1.17]	0.770	10/1649	2.52 [1.41–4.50]	**0.002**
dPVS (basal ganglia)		1.42 [0.73–2.73]	0.301		0.83 [0.35–1.93]	0.658		4.83 [1.07–21.92]	0.041
dPVS (white matter)		1.03 [0.60–1.80]	0.905		0.67 [0.33–1.36]	0.269		2.32 [0.63–8.47]	0.204
dPVS (hippocampus)		1.18 [1.02–1.36]	0.025		1.01 [0.84–1.22]	0.907		2.32 [1.53–3.50]	**7.09×10^{-5}**
dPVS (brain stem)		1.04 [0.92–1.18]	0.502		1.08 [0.94–1.24]	0.285		1.08 [0.79–1.47]	0.644
Model 5[e]									
dPVS (global)	66/1659	1.23 [1.05–1.43]	**0.010**	52/1659	1.03 [0.86–1.23]	0.728	10/1659	3.68 [1.95–6.96]	**5.81×10^{-5}**
dPVS (basal ganglia)		2.21 [1.24–3.93]	**0.007**		1.24 [0.58–2.66]	0.585		12.06 [3.26–44.56]	**0.0002**
dPVS (white matter)		1.19 [0.69–2.05]	0.531		0.75 [0.37–1.49]	0.410		3.38 [0.96–11.85]	0.058
dPVS (hippocampus)		1.23 [1.06–1.42]	**0.006**		1.03 [0.85–1.24]	0.769		2.88 [1.83–4.53]	**4.99×10^{-6}**
dPVS (brain stem)		1.06 [0.94–1.20]	0.365		1.08 [0.94–1.25]	0.253		1.14 [0.84–1.56]	0.400

dPVS (global) includes dPVS in basal ganglia (grade 3–4/1–2), white matter (grade 3–4/1–2), hippocampus (dPVS count, 0–5+), and brainstem (dPVS count, 0–6+); n/N, number of participants with stroke/total number of participants at risk, significance threshold after correction for multiple testing: $p < 0.0125$ are shown in bold.
Key: dPVS, dilated perivascular space.
[a] Model 1: adjusted for sex and intracranial volume;
[b] Model 2: as model 1, additionally adjusted for hypertension, diabetes mellitus, hypercholesterolemia, current smoking status, body mass index;
[c] Model 3: as model 1, additionally adjusted for APOE ε4 carrier status;
[d] Model 4: as model 1, additionally adjusted for white matter hyperintensities volume and covert MRI-defined lacunes;
[e] Model 5: as model 2, additionally adjusted for antithrombotic drug intake.

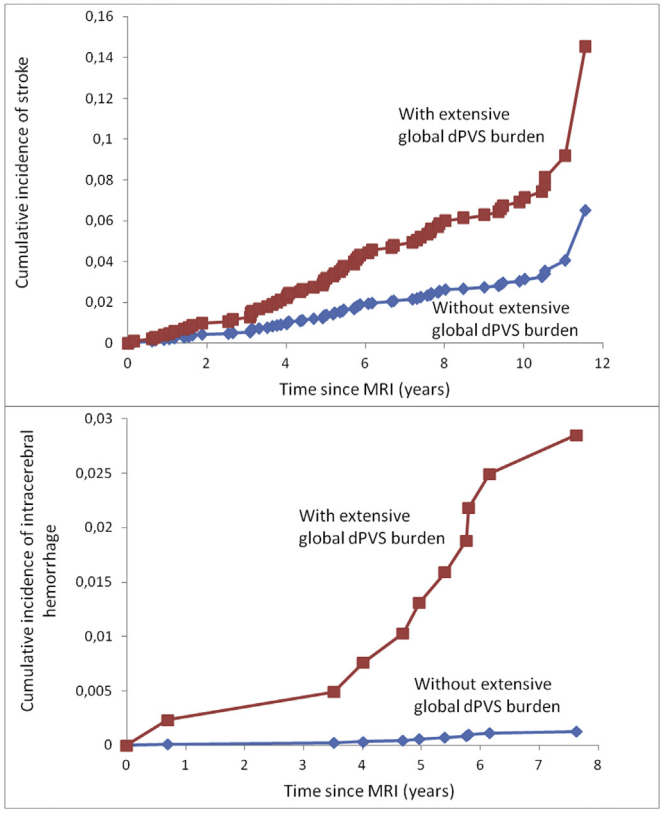

Fig. 2. Cumulative incidence of stroke and intracerebral hemorrhage based on age, sex, and total intracranial volume adjusted Cox models and stratified on global dPVS burden (extensive global dPVS burden [dPVS global score ≥7] vs. the rest). Abbreviations: dPVS, dilated perivascular space.

In a model accounting for age and adjusted for sex and ICV, higher global dPVS burden was associated with an increased risk of developing new strokes (Table 2; Fig. 2). Considering stroke subtypes, higher global dPVS burden was associated with an increased risk of ICH (Table 2; Fig. 2), but not ischemic stroke risk (overall and by individual subtypes). Higher dPVS burden in the BG and in the hippocampus were significantly associated with an increased risk of developing new strokes, and especially ICH, but not ischemic stroke (Table 2; Supplementary Table 1).

These associations remained substantially unchanged after further adjustment for vascular risk factors, antithrombotic drug intake, or APOEε4-carrier status. Higher burden of dPVSs in all locations and in the hippocampus, but not in the BG, was still associated with ICH risk after adjustment for other MRI-markers of cSVD (Table 2). The association between dPVSs in BG and ICH risk was no longer significant after adjustment for WMHV only (Supplementary Table 2). There was no deviation from linearity for the association with hippocampal dPVSs. We did not observe any significant association between dPVS burden in the WM or brainstem and incident stroke risk, although there was a nonsignificant trend ($p = 0.06–0.07$) toward an association of extensive dPVSs in the WM with increased risk of ICH (Table 2; Supplementary Table 1).

When testing the association of increasing dPVS grades in the BG with incident stroke, we found a significant trend test after correction for multiple testing, with increasing effect sizes for increasing BG dPVS grades (Table 3).

In secondary analyses, adjusting for brain parenchymal fraction instead of ICV did not change the results (Supplementary Table 3). We did not find any modifying effect of sex, hypertension, median age, or APOEε4-carrier status on the relationship of global dPVSs or dPVS subtypes with incident stroke (data not shown). Considering that most ICH cases in the general population are caused by cSVD, as is the small-artery occlusion ischemic stroke subtype, we ran secondary analyses combining these subtypes. Associations of dPVS burden in all locations, the hippocampus and the BG with this composite cSVD stroke phenotype were slightly more significant with narrower confidence intervals than for ICH alone (Supplementary Table 4). When testing the association of dPVS burden separately with incident fatal and nonfatal stroke, although results were not significant, slightly larger effect sizes were found for associations with fatal stroke (Supplementary Table 5).

4. Discussion

In a large population-based cohort study of 1678 persons aged 65+ years, we found a significant association between global dPVS burden and risk of incident ICH, but no association with incident ischemic stroke risk. A high dPVS burden in the BG and in the hippocampus was significantly associated with an increased risk of ICH, independent of vascular risk factors, antithrombotic drug intake, and APOEε4-carrier status, and also independent of other MRI markers of cSVD for dPVSs in the hippocampus.

In a recent population-based study of predominantly Hispanic origin (NOMAS, N = 1228), an association of a global dPVS burden score with any stroke risk was observed, only for participants in the highest tertile of blood pressure, in a model accounting for cofounders (Gutierrez et al., 2017). There was no association of dPVS burden in the WM, BG, brainstem, and posterior fossa with any

Table 3
Association between grades of dilated perivascular spaces in basal ganglia and incident stroke

	All strokes											
	Model 1[a]			Model 2[b]			Model 3[c]			Model 4[d]		
	n/N	HR [95% CI]	*p* for trend	n/N	HR [95% CI]	*p* for trend	n/N	HR [95% CI]	*p* for trend	n/N	HR [95% CI]	*p* for trend
dPVS (basal ganglia)			**0.002**			**0.003**			**0.002**			0.205
Grade 1	25/916	Referent		25/906	Referent		25/911	Referent		25/905	Referent	
Grade 2	25/581	1.49 [0.86–2.61]		25/574	1.47 [0.84–2.57]		25/575	1.50 [0.86–2.61]		25/570	1.30 [0.74–2.29]	
Grade 3	14/161	2.70 [1.39–5.24]		14/159	2.61 [1.33–5.09]		14/160	2.68 [1.38–5.21]		14/156	1.68 [0.79–3.55]	
Grade 4	2/20	3.04 [0.71–13.01]		2/20	3.23 [0.75–13.91]		2/20	3.08 [0.72–13.18]		2/18	1.39 [0.29–6.60]	

n/N, number of participants with stroke/total number of participants at risk, significance threshold: $p < 0.05$ are shown in bold.
Key: dPVS, dilated perivascular space.
[a] Model 1: adjusted for sex and intracranial volume;
[b] Model 2: as model 1, additionally adjusted for hypertension, diabetes mellitus, hypercholesterolemia, current smoking status, body mass index;
[c] Model 3: as model 1, additionally adjusted for APOE ε4 carrier status;
[d] Model 4: as model 1, additionally adjusted for white matter hyperintensities volume and covert MRI-defined lacunes.

stroke risk. Despite a similar age of both study populations, the burden of dPVS seemed to be less in NOMAS than in 3C-Dijon (9% of the NOMAS population had a dPVS score of 0 vs. none in the 3C-Dijon study), possibly related to ethnic differences, lower blood pressure in NOMAS, and variations in dPVS detection and scoring (Lau et al., 2017). The somewhat smaller sample size in NOMAS may also have contributed to the absence of significant association of dPVS burden with incident stroke (Gutierrez et al., 2017). Moreover, importantly, neither dPVSs in the hippocampus, nor stroke subtypes were considered in the NOMAS study.

In 2 high-risk populations with a history of ischemic stroke or transient ischemic attack (total N = 2002), from the UK (OXVASC) and China (HKU), high dPVS burden in the BG, but not in the WM, was associated with higher risk of recurrent all stroke and ischemic stroke, but not ICH (Lau et al., 2017). However, all participants in this population had a history of cerebral ischemia and were therefore at particularly high risk of ischemic stroke versus ICH. Finally, in a study carried out in 229 cerebral amyloid angiopathy (CAA)-related ICH patients, high dPVS burden in the WM ($\geq$20 dPVSs) was associated with an increased risk of ICH recurrence (other dPVS locations were not examined) (Boulouis et al., 2017).

In the present study, the association of dPVS burden with risk of stroke and stroke subtypes differed according to the dPVS location, the most significant associations being observed with dPVSs in the BG and hippocampus. Patterns of association of dPVS burden with risk factors differ depending on dPVS location. dPVSs in the BG are more strongly associated with hypertension (Yang et al., 2017; Zhu et al., 2010a) and blood pressure variability (Yang et al., 2017) than dPVSs in the WM, while the latter show stronger correlations with Alzheimer's disease (Banerjee et al., 2017; Ramirez, 2015; Roher et al., 2003) and CAA (Charidimou et al., 2017). This, together with the strong association of high blood pressure levels and antihypertensive treatment with dPVS burden in our sample, and considering the well-established major effect of hypertension on stroke risk, which is even stronger for ICH than for ischemic stroke (O'Donnell et al., 2010), could suggest that the observed association between dPVS burden and incident stroke could partly reflect the effect of hypertension on both. However, associations were maintained after adjusting for hypertension and other vascular risk factors, suggesting that other mechanisms are at play, although some degree of residual confounding cannot be excluded.

The particularly strong association of dPVS burden with incident ICH is intriguing. It is consistent with previous reports showing that MRI markers of cSVD, even if not hemorrhagic in nature, such as WMH or covert MRI-defined lacunes, are associated with an increased risk of ICH (Folsom et al., 2012; Kaffashian et al., 2016; Windham et al., 2015). This highlights the importance of assessing the benefit-risk ratio of antiplatelet agents in persons with covert cSVD (frequently prescribed empirically in clinical practice) in a randomized clinical trial setting. The similar effect estimates for associations of dPVS burden with incident small-artery occlusion ischemic stroke, with enhanced significance when combining with incident ICH, are also in favor of effects mediated by cSVD. A direct topographical association has been described between juxtacortical dPVSs and CAA severity in the cortex, in the specific context of Alzheimer's disease patients with CAA (Veluw et al., 2016). The population-based setting of our study and the relatively small number of incident ICH cases did not enable us to explore the associations of dPVS burden with lobar versus nonlobar ICH. Interestingly, cross-sectional studies have described a higher prevalence of dPVSs in the BG in patients with ICH in deep structures and of WM dPVSs in patients with lobar ICH (Charidimou et al., 2017). This observation is in line with the stronger correlation of BG dPVSs with hypertension (Yang et al., 2017; Zhu et al., 2010a), and of WM dPVSs with CAA (Charidimou et al., 2017; Veluw et al., 2016), as deep ICH is more often caused by hypertension and lobar ICH by CAA (Graff-Radford et al., 2017; Greenberg et al., 2009).

We can hypothesize that some of the mechanisms underlying the association between dPVS burden and stroke, especially for dPVSs in the BG, are common with the other MRI markers of cSVD, particularly with WMHV (Kaffashian et al., 2016). Indeed, associations with BG dPVSs were attenuated and only nominally significant after adjusting for WMHV. Corroborating this, we recently described a strong phenotypic and genetic correlation between dPVSs in BG and WMHV (Duperron et al., 2018). However, interestingly, the association of hippocampal dPVS burden with incident stroke and ICH was independent of other MRI markers of cSVD, suggesting that other mechanisms may be involved here. dPVSs and WMH colocalize spatially, with WMH appearing around dPVSs (Wardlaw et al., 2013a); however, this is not the case of the hippocampus that consists almost exclusively of gray matter; this distinctive feature could perhaps partly explain that the associations with hippocampal dPVSs remain independent of other cSVD features, measured primarily in the WM. Although they have common risk factors with dPVSs in BG and WM, dPVSs in hippocampus may differ from the other locations as it has been suggested that they may at least in part result from incomplete fusion of the hippocampus fissure during development (Yao et al., 2014).

dPVSs may reflect "glymphatic" fluid stasis and play a role in the pathogenesis of cSVD (Jessen et al., 2015; Mestre et al., 2017). dPVS dilatation could be the consequence of blood-brain barrier dysfunction, arterial wall stiffening, or endothelial cell disconnection, and involve microglial cells and perivascular macrophages (Faraco et al., 2016; Ramirez et al., 2016). Perivascular macrophages, a specific population of resident brain macrophages located in dPVSs, have a pathogenic role in neurovascular and cognitive function associated with hypertension, in particular by generating large amounts of reactive oxygen species, which may lead to blood-brain barrier disruption (Faraco et al., 2016). Interestingly ICH patients have high levels of oxidative stress (Gonullu et al., 2014).

Strengths of our study include the population-based setting and longitudinal design with a large sample size, stroke classification, and validation by an expert panel, and rating of dPVSs by the same experienced reader on 3D-T1 images with differentiation from WMH and covert MRI-defined lacunes using careful examination in the 3 planes and exploration of T2 and PD sequences. Although the resolution in later generation 7T MRI scanners is higher, smaller PVS that are not detectable on 1.5 T scanners may perhaps reflect physiological rather than pathological processes. Our study has limitations. dPVSs were rated on a visual scale, and although intrarater agreement was good (Zhu et al., 2010a), automated dPVS quantification scales would provide more reproducible measures; however, such software are not yet available. Caution is warranted when interpreting effect sizes given the relatively small number of ICH cases, confirmation in independent samples is required. Participants included in the analysis were on average younger and had fewer vascular risk factors than 3C-Dijon participants not included (Supplementary Table 6), which may have led to underestimated results. Presence of cerebral microbleeds was shown to be associated with increased risk of ischemic stroke and ICH (Debette et al., 2019; Wilson et al., 2016), and cortical superficial siderosis was found to be associated with incident ICH (Wollenweber et al., 2019). Unfortunately, the 3C-Dijon study brain imaging protocol from 1999 did not include any T2* images, hence we were unable to assess the impact of cerebral microbleeds and cortical superficial siderosis on the association between dPVS burden and incident stroke.

5. Conclusions

Our findings, if confirmed in independent samples, imply that dPVS burden in the BG and in the hippocampus may be a strong MRI marker of incident ICH risk, providing novel insight into the clinical significance of dPVSs and regional variations thereof.

Disclosure

All authors report no disclosure.

Acknowledgements

The authors thank the participants of the 3C study for their important contributions. The 3-City Study is conducted under a partnership agreement among INSERM, Univ. Bordeaux, and Sanofi-Aventis. The Fondation pour la Recherche Médicale funded the preparation and initiation of the study. The 3C Study is supported by the Caisse Nationale Maladie des Travailleurs Salariés, Direction Générale de la Santé, Mutuelle Générale de l'Education Nationale, Institut de la Longévité, Conseils Régionaux of Aquitaine and Bourgogne, Fondation de France, and Ministry of Research–INSERM Programme "Cohortes et collections de données biologiques." Stéphanie Debette is supported by the European Research Council, European Union, and a grant from the Joint Programme of Neurodegenerative Disease research, from the European Union's Horizon 2020 research and innovation programme under grant agreements (No 643417, No 667375 & No 640643), by the Initiative of Excellence of Bordeaux University, and the Agence Nationale pour le Recherche.

Appendix A. Supplementary data

Supplementary data to this article can be found online at https://doi.org/10.1016/j.neurobiolaging.2019.08.031.

References

Bacyinski, A., Xu, M., Wang, W., Hu, J., 2017. The paravascular pathway for brain waste clearance: current understanding, significance and controversy. Front Neuroanat. 11, 101.

Banerjee, G., Kim, H.J., Fox, Z., Jäger, H.R., Wilson, D., Charidimou, A., Na, H.K., Na, D.L., Seo, S.W., Werring, D.J., 2017. MRI-visible perivascular space location is associated with Alzheimer's disease independently of amyloid burden. Brain 140, 1107–1116.

Boulouis, G., Charidimou, A., Pasi, M., Roongpiboonsopit, D., Xiong, L., Auriel, E., van Etten, E.S., Martinez-Ramirez, S., Ayres, A., Vashkevich, A., Schwab, K.M., Rosand, J., Goldstein, J.N., Gurol, M.E., Greenberg, S.M., Viswanathan, A., 2017. Hemorrhage recurrence risk factors in cerebral amyloid angiopathy: comparative analysis of the overall small vessel disease severity score versus individual neuroimaging markers. J. Neurol. Sci. 380, 64–67.

Charidimou, A., Boulouis, G., Pasi, M., Auriel, E., Etten, E.S., Haley, K., Ayres, A., Schwab, K.M., Martinez-Ramirez, S., Goldstein, J.N., Rosand, J., Viswanathan, A., Greenberg, S.M., Gurol, M.E., 2017. MRI-visible perivascular spaces in cerebral amyloid angiopathy and hypertensive arteriopathy. Neurology 88, 1157–1164.

Debette, S., Schilling, S., Duperron, M.G., Larsson, S.C., Markus, H.S., 2019. Clinical significance of magnetic resonance imaging markers of vascular brain Injury: a systematic review and meta-analysis. JAMA Neurol. 76, 81–94.

Desquilbet, L., Mariotti, F., 2010. Dose-response analyses using restricted cubic spline functions in public health research. Stat. Med. 29, 1037–1057.

Duperron, M.G., Tzourio, C., Sargurupremraj, M., Mazoyer, B., Soumare, A., Schilling, S., Amouyel, P., Chauhan, G., Zhu, Y.C., Debette, S., 2018. Burden of dilated perivascular spaces, an emerging marker of cerebral small vessel disease, is highly heritable. Stroke 49, 282–287.

Faraco, G., Sugiyama, Y., Lane, D., Garcia-Bonilla, L., Chang, H., Santisteban, M.M., Racchumi, G., Murphy, M., Rooijen, N.V., Anrather, J., Iadecola, C., 2016. Perivascular macrophages mediate the neurovascular and cognitive dysfunction associated with hypertension. J. Clin. Invest. 126, 4674.

Folsom, A.R., Yatsuya, H., Mosley Jr., T.H., Psaty, B.M., Longstreth Jr., W.T., 2012. Risk of intraparenchymal hemorrhage with magnetic resonance imaging-defined leukoaraiosis and brain infarcts. Ann. Neurol. 71, 552–559.

Francis, F., Ballerini, L., Wardlaw, J.M., 2019. Perivascular spaces and their associations with risk factors, clinical disorders and neuroimaging features: a systematic review and meta-analysis. Int. J. Stroke 14, 359–371.

Gonullu, H., Aslan, M., Karadas, S., Kat, C., Duran, L., Milanlioglu, A., Aydin, M.N., Demir, H., 2014. Serum prolidase enzyme activity and oxidative stress levels in patients with acute hemorrhagic stroke. Scand. J. Clin. Lab. Invest. 74, 199–205.

Graff-Radford, J., Simino, J., Kantarci, K., Mosley, T.H., Griswold, M.E., Windham, B.G., Sharrett, A.R., Albert, M.S., Gottesman, R.F., Jack, C.R., Vemuri, P., Knopman, D.S., 2017. Neuroimaging correlates of cerebral microbleeds: the ARIC study (atherosclerosis risk in communities). Stroke 48, 2964–2972.

Greenberg, S.M., Vernooij, M.W., Cordonnier, C., Viswanathan, A., Al-Shahi Salman, R., Warach, S., Launer, L.J., Van Buchem, M.A., Breteler, M.M., Microbleed Study, G., 2009. Cerebral microbleeds: a guide to detection and interpretation. Lancet Neurol. 8, 165–174.

Gutierrez, J., Elkind, M.S.V., Dong, C., Di Tullio, M., Rundek, T., Sacco, R.L., Wright, C.B., 2017. Brain perivascular spaces as biomarkers of vascular risk: results from the Northern Manhattan study. AJNR. Am. J. Neuroradiol. 38, 862–867.

Jessen, N.A., Munk, A.S.F., Lundgaard, I., Nedergaard, M., 2015. The glymphatic system: a beginner's guide. Neurochem. Res. 40, 2583–2599.

Kaffashian, S., Tzourio, C., Zhu, Y.C., Mazoyer, B., Debette, S., 2016. Differential effect of white-matter lesions and covert brain infarcts on the risk of ischemic stroke and intracerebral hemorrhage. Stroke 47, 1923–1925.

Kwee, R.M., Kwee, T.C., 2007. Virchow-robin spaces at MR imaging. Radiographics 27, 1071–1086.

Lau, K.-K., Li, L., Lovelock, C.E., Zamboni, G., Chan, T.-T., Chiang, M.-F., Lo, K.-T., Küker, W., Mak, H.K., Rothwell, P.M., 2017. Clinical correlates, ethnic differences, and prognostic implications of perivascular spaces in transient ischemic attack and ischemic stroke. Stroke 48, 1470–1477.

Lemaitre, H., Crivello, F., Grassiot, B., Alperovitch, A., Tzourio, C., Mazoyer, B., 2005. Age- and sex-related effects on the neuroanatomy of healthy elderly. Neuroimage 26, 900–911.

Maillard, P., Delcroix, N., Crivello, F., Dufouil, C., Gicquel, S., Joliot, M., Tzourio-Mazoyer, N., Alperovitch, A., Tzourio, C., Mazoyer, B., 2008. An automated procedure for the assessment of white matter hyperintensities by multispectral (T1, T2, PD) MRI and an evaluation of its between-centre reproducibility based on two large community databases. Neuroradiology 50, 31–42.

MacLullich, A., Wardlaw, J., Ferguson, K., Starr, J., Seckl, J., Deary, I., 2004. Enlarged perivascular spaces are associated with cognitive function in healthy elderly men. J. Neurol. Neurosurg. Psychiatry 75, 1519.

Mestre, H., Kostrikov, S., Mehta, R.I., Nedergaard, M., 2017. Perivascular spaces, glymphatic dysfunction, and small vessel disease. Clin. Sci. (Lond) 131, 2257–2274.

O'Donnell, M.J., Xavier, D., Liu, L., Zhang, H., Chin, S.L., Rao-Melacini, P., Rangarajan, S., Islam, S., Pais, P., McQueen, M.J., Mondo, C., Damasceno, A., Lopez-Jaramillo, P., Hankey, G.J., Dans, A.L., Yusoff, K., Truelsen, T., Diener, H.C., Sacco, R.L., Ryglewicz, D., Czlonkowska, A., Weimar, C., Wang, X., Yusuf, S., Investigators, I., 2010. Risk factors for ischaemic and intracerebral haemorrhagic stroke in 22 countries (the INTERSTROKE study): a case-control study. Lancet 376, 112–123.

Passiak, B.S., Liu, D., Kresge, H.A., Cambronero, F.E., Pechman, K.R., Osborn, K.E., Gifford, K.A., Hohman, T.J., Schrag, M.S., Davis, L.T., Jefferson, A.L., 2019. Perivascular spaces contribute to cognition beyond other small vessel disease markers. Neurology 92, e1309–e1321.

Potter, G.M., Doubal, F.N., Jackson, C.A., Chappell, F.M., Sudlow, C.L., Dennis, M.S., Wardlaw, J.M., 2015. Enlarged perivascular spaces and cerebral small vessel disease. Int. J. Stroke 10, 376–381.

Ramirez, J., Berezuk, C., McNeely, A.A., Gao, F., McLaurin, J., Black, S.E., 2016. Imaging the perivascular space as a potential biomarker of neurovascular and neurodegenerative diseases. Cell Mol. Neurobiol. 36, 289–299.

Ramirez, J.B., Courtney, McNeely, A.A., Scott, C.J.M., Gao, F., Black, S.E., 2015. Visible virchow-robin spaces on magnetic resonance imaging of Alzheimer's disease patients and normal elderly from the sunnybrook dementia study. J. Alzheimers Dis. 43, 415–424.

Roher, A.E., Kuo, Y.-M., Esh, C., Knebel, C., Weiss, N., Kalback, W., Luehrs, D.C., Childress, J.L., Beach, T.G., Weller, R.O., Kokjohn, T.A., 2003. Cortical and leptomeningeal cerebrovascular amyloid and white matter pathology in Alzheimer's disease. Mol. Med. 9, 112.

The 3C-Study Group, 2003. Vascular factors and risk of dementia: design of the three-city study and baseline characteristics of the study population. Neuroepidemiology 22, 316–325.

Veluw, S.J.V., Biessels, G.J., Bouvy, W.H., Spliet, W.G., Zwanenburg, J.J., Luijten, P.R., Macklin, E.A., Rozemuller, A.J., Gurol, M.E., Greenberg, S.M., Viswanathan, A., Martinez-Ramirez, S., 2016. Cerebral amyloid angiopathy severity is linked to dilation of juxtacortical perivascular spaces. J. Cereb. Blood Flow Metab. 36, 576–580.

Verhaaren, B.F., Debette, S., Bis, J.C., Smith, J.A., Ikram, M.K., Adams, H.H., Beecham, A.H., Rajan, K.B., Lopez, L.M., Barral, S., van Buchem, M.A., van der Grond, J., Smith, A.V., Hegenscheid, K., Aggarwal, N.T., de Andrade, M., Atkinson, E.J., Beekman, M., Beiser, A.S., Blanton, S.H., Boerwinkle, E., Brickman, A.M., Bryan, R.N., Chauhan, G., Chen, C.P., Chouraki, V., de Craen, A.J., Crivello, F., Deary, I.J., Deelen, J., De Jager, P.L., Dufouil, C., Elkind, M.S., Evans, D.A., Freudenberger, P., Gottesman, R.F., Guethnason, V., Habes, M., Heckbert, S.R., Heiss, G., Hilal, S., Hofer, E., Hofman, A., Ibrahim-Verbaas, C.A., Knopman, D.S., Lewis, C.E., Liao, J., Liewald, D.C., Luciano, M., van der Lugt, A.,

Martinez, O.O., Mayeux, R., Mazoyer, B., Nalls, M., Nauck, M., Niessen, W.J., Oostra, B.A., Psaty, B.M., Rice, K.M., Rotter, J.I., von Sarnowski, B., Schmidt, H., Schreiner, P.J., Schuur, M., Sidney, S.S., Sigurdsson, S., Slagboom, P.E., Stott, D.J., van Swieten, J.C., Teumer, A., Toglhofer, A.M., Traylor, M., Trompet, S., Turner, S.T., Tzourio, C., Uh, H.W., Uitterlinden, A.G., Vernooij, M.W., Wang, J.J., Wong, T.Y., Wardlaw, J.M., Windham, B.G., Wittfeld, K., Wolf, C., Wright, C.B., Yang, Q., Zhao, W., Zijdenbos, A., Jukema, J.W., Sacco, R.L., Kardia, S.L., Amouyel, P., Mosley, T.H., Longstreth Jr., W.T., DeCarli, C.C., van Duijn, C.M., Schmidt, R., Launer, L.J., Grabe, H.J., Seshadri, S.S., Ikram, M.A., Fornage, M., 2015. Multiethnic genome-wide association study of cerebral white matter hyperintensities on MRI. Circ. Cardiovasc. Genet. 8, 398–409.

Wardlaw, J.M., Smith, C., Dichgans, M., 2013a. Mechanisms of sporadic cerebral small vessel disease: insights from neuroimaging. Lancet Neurol. 12, 483–497.

Wardlaw, J.M., Smith, E.E., Biessels, G.J., Cordonnier, C., Fazekas, F., Frayne, R., Lindley, R.I., O'Brien, J.T., Barkhof, F., Benavente, O.R., Black, S.E., Brayne, C., Breteler, M., Chabriat, H., DeCarli, C., de Leeuw, F.-E., Doubal, F., Duering, M., Fox, N.C., Greenberg, S., Hachinski, V., Kilimann, I., Mok, V., Oostenbrugge, R.V., Pantoni, L., Speck, O., Stephan, B.C.M., Teipel, S., Viswanathan, A., Werring, D., Chen, C., Smith, C., van Buchem, M., Norrving, B., Gorelick, P.B., Dichgans, M., 2013b. Neuroimaging standards for research into small vessel disease and its contribution to ageing and neurodegeneration. Lancet Neurol. 12, 822–838.

WHO MONICA Project Principal Investigators, 1988. The World Health Organization MONICA Project (monitoring trends and determinants in cardiovascular disease): a major international collaboration. J. Clin. Epidemiol. 41, 105–114.

Wilson, D., Charidimou, A., Ambler, G., Fox, Z.V., Gregoire, S., Rayson, P., Imaizumi, T., Fluri, F., Naka, H., Horstmann, S., Veltkamp, R., Rothwell, P.M., Kwa, V.I., Thijs, V., Lee, Y.S., Kim, Y.D., Huang, Y., Wong, K.S., Jager, H.R., Werring, D.J., 2016. Recurrent stroke risk and cerebral microbleed burden in ischemic stroke and TIA: a meta-analysis. Neurology 87, 1501–1510.

Windham, B.G., Deere, B., Griswold, M.E., Wang, W., Bezerra, D.C., Shibata, D., Butler, K., Knopman, D., Gottesman, R.F., Heiss, G., Mosley, T.H., 2015. Small brain lesions and incident stroke and mortality: a cohort study. Ann. Intern. Med. 163, 22.

Wollenweber, F.A., Opherk, C., Zedde, M., Catak, C., Malik, R., Duering, M., Konieczny, M.J., Pascarella, R., Samoes, R., Correia, M., Marti-Fabregas, J., Linn, J., Dichgans, M., 2019. Prognostic relevance of cortical superficial siderosis in cerebral amyloid angiopathy. Neurology 92, e792–e801.

Yakushiji, Y., Charidimou, A., Hara, M., Noguchi, T., Nishihara, M., Eriguchi, M., Nanri, Y., Nishiyama, M., Werring, D.J., Hara, H., 2014. Topography and associations of perivascular spaces in healthy adults: the Kashima scan study. Neurology 83, 2116–2123.

Yang, S., Qin, W., Yang, L., Fan, H., Li, Y., Yin, J., Hu, W., 2017. The relationship between ambulatory blood pressure variability and enlarged perivascular spaces: a cross-sectional study. BMJ Open 7, e015719.

Yao, M., Zhu, Y.-C., Soumaré, A., Dufouil, C., Mazoyer, B., Tzourio, C., Chabriat, H., 2014. Hippocampal perivascular spaces are related to aging and blood pressure but not to cognition. Neurobiol. Aging 35, 2118–2125.

Zhu, Y.-C., Tzourio, C., Soumaré, A., Mazoyer, B., Dufouil, C., Chabriat, H., 2010a. Severity of dilated Virchow-Robin spaces is associated with age, blood pressure, and MRI markers of small vessel disease: a population-based study. Stroke 41, 2483–2490.

Zhu, Y.-C., Dufouil, C., Soumaré, A., Mazoyer, B., Chabriat, H., Tzourio, C., 2010b. High degree of dilated Virchow-Robin spaces on MRI is associated with increased risk of dementia. J. Alzheimers Dis. 22, 663–672.